

Non-divergent pseudo-potential treatment of spin-polarized fermions under 1D and 3D harmonic confinement

K. Kanjilal and D. Blume¹

¹*Department of Physics, Washington State University, Pullman, WA 99164-2814*

Atom-atom scattering of bosonic one-dimensional (1D) atoms has been modeled successfully using a zero-range delta-function potential, while that of bosonic 3D atoms has been modeled successfully using Fermi-Huang's regularized s -wave pseudo-potential. Here, we derive the eigenenergies of two spin-polarized 1D fermions under external harmonic confinement interacting through a zero-range potential, which only acts on odd-parity wave functions, analytically. We also present a divergent-free zero-range potential treatment of two spin-polarized 3D fermions under harmonic confinement. Our pseudo-potential treatments are verified through numerical calculations for short-range model potentials.

PACS numbers: 34.50.-s, 34.10.+x

I. INTRODUCTION

Recently, atom-atom scattering has received renewed interest since the properties of ultracold atomic (bosonic or fermionic) gases depend predominantly on a single atom-atom scattering parameter [1]. This is the s -wave scattering length a_s for a three-dimensional (3D) Bose gas [2] (or for a 3D Fermi gas consisting of atoms with “spin-up” and “spin-down”), and the p -wave scattering volume V_p [3, 4] for a 3D spin-polarized Fermi gas. For a 1D or quasi-1D gas, it is the 1D scattering length a_{1D} [5, 6], which characterizes the even-parity and odd-parity spatial wave function applicable to bosons and to spin-polarized fermions, respectively. In many instances, atom-atom scattering processes can be conveniently modeled through a shape-independent pseudo-potential [7, 8], whose coupling strength is chosen such that it reproduces the scattering properties of the full shape-dependent 3D or 1D atom-atom potential.

Fermi-Huang's regularized pseudo-potential [9, 10, 11] supports a single bound state for positive a_s and no bound state for negative a_s . It has been used frequently to describe 3D s -wave scattering between two bosons or two fermions with different generalized spin. Busch *et al.* [12], e.g., derive the eigenenergies for two atoms under harmonic confinement interacting through Fermi Huang's pseudo-potential analytically. Using an energy-dependent scattering length $a_s(E)$, their results can be applied successfully to situations where a_s is large and positive, i.e., near a Feshbach resonance [13, 14, 15]. Building on these results, Borca *et al.* [16] use a simple two-atom model to explain many aspects of an experiment that produces molecules from a sea of cold atoms using magnetic field ramps [17]. In addition to these two-body applications, Fermi-Huang's 3D s -wave pseudo-potential plays a key role in developing (effective) many-body theories.

This paper determines the eigenspectrum of two spin-polarized 3D fermions interacting through a regularized p -wave zero-range potential, parameterized through a *single parameter*, i.e., the p -wave scattering volume V_p , under harmonic confinement analytically. Since wave functions with relative angular momentum l greater than zero have vanishing amplitude at $r = 0$ (where r denotes the distance between the

two atoms), our zero-range p -wave potential contains derivative operators. Furthermore, it contains, following ideas suggested by Huang and Yang in 1957 [11], a so-called regularization operator, which eliminates divergencies at $r = 0$ that would arise otherwise. We show that our pseudo-potential imposes a boundary condition on the wave function at $r = 0$ (see also Ref. [18]); this boundary condition serves as an alternative representation of the p -wave pseudo-potential. Earlier studies, in contrast, impose a boundary condition at finite r , corresponding to a *finite-range* pseudo-potential with *two parameters* [19, 20]. The validity of our pseudo-potential is demonstrated by comparing the eigenenergies determined analytically for two particles under harmonic confinement with those determined numerically for shape-dependent atom-atom potentials.

Due to significant advancements in trapping and cooling, to date cold atomic gases cannot only be trapped in 3D geometries but also in quasi-2D and quasi-1D geometries [21, 22, 23]. In the quasi-1D regime, the transverse motion is “frozen out” so that the behaviors of atomic gases are dominated by the longitudinal motion. Quasi-1D gases can hence often be treated within a 1D model, where the atoms are restricted to a line. To model 1D atom-atom interactions, for which the spatial wave function has *even parity*, delta-function contact interactions have been used successfully. In contrast to the 3D s -wave delta-function potential, which requires a regularization, the 1D delta-function pseudo-potential is non-divergent [24]. To treat spin-polarized 1D fermions, a pseudo-potential that acts on spatial wave functions with *odd parity* is needed. Here, we use such a pseudo-potential to determine the eigenenergies of two spin-polarized 1D fermions under harmonic confinement analytically. Comparison with eigenenergies determined numerically for shape-dependent 1D atom-atom potentials illustrates the applicability of our 1D pseudo-potential. Our results confirm the Fermi-Bose duality [25, 26, 27, 28, 29] in 1D for two atoms under harmonic confinement.

II. TWO INTERACTING 1D PARTICLES UNDER HARMONIC CONFINEMENT

Consider two 1D atoms with mass m and coordinates z_1 and z_2 , respectively, under external harmonic confinement,

$$V_{rap}(z_1, z_2) = \frac{1}{2}m\omega_z^2(z_1^2 + z_2^2), \quad (1)$$

where ω_z denotes the angular frequency. After separating the center of mass and the relative motion, the Schrödinger equation for the relative degree of freedom z , where $z = z_2 - z_1$, reads

$$H_{1D}\Psi_{1D}(z) = E_{1D}\Psi_{1D}(z), \quad (2)$$

where

$$H_{1D} = -\frac{\hbar^2}{2\mu} \frac{d^2}{dz^2} + V(z) + \frac{1}{2}\mu\omega_z^2 z^2. \quad (3)$$

Here, $V(z)$ denotes the 1D atom-atom interaction potential, and μ the reduced mass, $\mu = m/2$.

Section II A reviews the pseudo-potential treatment of two 1D particles with even-parity eigenstates, i.e., two bosons or two fermions with opposite spin, under harmonic confinement. Section II B determines the relative eigenenergies E_{1D}^- for two spin-polarized 1D fermions interacting through a momentum-dependent zero-range potential under harmonic confinement analytically. Section II C benchmarks our treatment of the momentum-dependent zero-range potential by comparing with numerical results obtained for a short-range model potential.

A. Review of pseudo-potential treatment: Even parity

The relative eigenenergies E_{1D}^+ corresponding to states with even parity (in the following referred to as even-parity eigenenergies) of two 1D particles interacting through the zero-range pseudo-potential $V_{pseudo}^+(z)$, where

$$V_{pseudo}^+(z) = \hbar\omega_z g_{1D}^+ \delta^{(1)}(z), \quad (4)$$

have been determined by Busch *et al.* [12]:

$$\frac{g_{1D}^+}{a_z} = -\frac{2\Gamma(-\frac{E_{1D}^+}{2\hbar\omega_z} + \frac{3}{4})}{\Gamma(-\frac{E_{1D}^+}{2\hbar\omega_z} + \frac{1}{4})}. \quad (5)$$

In Eq. (4), $\delta^{(1)}(z)$ denotes the usual 1D delta function. The transcendental equation (5) allows the coupling strength g_{1D}^+ for a given energy E_{1D}^+ to be determined readily. Vice versa, for a given g_{1D}^+ , the even-parity eigenenergies E_{1D}^+ can be determined semi-analytically. Figure 1(a) shows the resulting eigenenergies E_{1D}^+ of two 1D bosons or two 1D fermions with opposite spin as a function of the coupling strength g_{1D}^+ . As expected, for vanishing interaction strength ($g_{1D}^+ = 0$), the relative energies E_{1D}^+ coincide with the harmonic oscillator eigenenergies E_n^{osc} with even parity, $E_n^{osc} = (2n + \frac{1}{2})\hbar\omega_z$, where $n = 0, 1, \dots$.

For $|E_{1D}^+| \rightarrow \infty$ (and correspondingly negative g_{1D}^+), Eq. (5) reduces to lowest order to

$$E_{1D}^+ = -\frac{\hbar^2}{2\mu(a_{1D}^+)^2}, \quad (6)$$

which coincides with the exact binding energy of the pseudo-potential $V_{pseudo}^+(z)$ without confining potential. In Eq. (6), a_{1D}^+ denotes the 1D even-parity scattering length,

$$a_{1D}^+ = \lim_{k \rightarrow 0} -\frac{\tan(\delta_{1D}^+(k))}{k}, \quad (7)$$

which is related to the 1D coupling constant g_{1D}^+ through

$$a_{1D}^+ = -\frac{1}{g_{1D}^+}. \quad (8)$$

In Eq. (7), k denotes the relative 1D wave vector, $k = \sqrt{2\mu E_{sc}}/\hbar$, and E_{sc} the 1D scattering energy. The phase shift δ_{1D}^+ is obtained by matching the free-space scattering solution for positive z to $\sin(kz + \delta_{1D}^+)$. The dashed line in Fig. 1(a) shows the binding energy of the even-parity pseudo-potential without confinement, Eq. (6), while the dash-dotted line shows the expansion of Eq. (5) to next higher order.

In addition to the 1D eigenenergies E_{1D}^+ , the eigenfunctions $\Psi_{1D}^+(z)$ can be determined analytically, resulting in the logarithmic derivative

$$\left[\frac{d\Psi_{1D}^+(z)}{dz} \right]_{z \rightarrow 0^+} = \frac{g_{1D}^+}{a_z^2}. \quad (9)$$

This boundary condition is an alternative representation of the even-parity pseudo-potential $V_{pseudo}^+(z)$.

B. Analytical pseudo-potential treatment: Odd parity

Following the derivation of the even-parity eigenenergies by Busch *et al.* [12], we now derive an analogous expression for the odd-parity eigenenergies E_{1D}^- using the zero-range pseudo-potential $V_{pseudo}^-(z)$,

$$V_{pseudo}^-(z) = \hbar\omega_z g_{1D}^- \frac{\leftarrow d}{dz} \delta^{(1)}(z) \frac{d \rightarrow}{dz}. \quad (10)$$

This pseudo-potential leads to discontinuous eigenfunctions with continuous derivatives at $z = 0$. We show that the logarithmic derivative of $\Psi_{1D}^-(z)$ is well-behaved for $z \rightarrow 0^+$. In Eq. (10), the first derivative acts to the left and the second to the right,

$$\int_{-\infty}^{\infty} \phi^*(z) V_{pseudo}^-(z) \chi(z) dz = \hbar\omega_z g_{1D}^- \frac{d\phi^*(0)}{dz} \frac{d\chi(0)}{dz}, \quad (11)$$

with the short-hand notation

$$\frac{d\chi(0)}{dz} = \left[\frac{d\chi(z)}{dz} \right]_{z=0}. \quad (12)$$

Since $V_{pseudo}^-(z)$ acts only on wave functions with odd parity (and not on those with even parity), we refer to $V_{pseudo}^-(z)$ as odd-parity pseudo-potential; however, $V_{pseudo}^-(z)$ itself has even parity. Similar pseudo-potentials have recently also been used by others [28, 29, 30].

To start with, we expand the *discontinuous* odd-parity eigenfunction $\psi_{1D}^-(z)$ in *continuous* 1D odd-parity harmonic oscillator eigenfunctions $\phi_n(z)$,

$$\Psi_{1D}^-(z) = \sum_{n=0}^{\infty} c_n \phi_n(z), \quad (13)$$

where the c_n denote expansion coefficients, and

$$\phi_n(z) = \sqrt{\frac{2}{L_n^{(1/2)}(0)\sqrt{\pi}a_z}} \frac{z}{a_z} \exp\left(-\frac{z^2}{2a_z^2}\right) L_n^{(1/2)}\left(\frac{z^2}{a_z^2}\right), \quad (14)$$

where $a_z = \sqrt{\hbar/(\mu\omega_z)}$. In Eq. (14), the $L_n^{(1/2)}(z^2/a_z^2)$ denote associated Laguerre polynomials and the $\phi_n(z)$ are normalized to one,

$$\int_{-\infty}^{\infty} |\phi_n(z)|^2 dz = 1. \quad (15)$$

The corresponding odd-parity harmonic oscillator eigenenergies are

$$E_n^{osc} = \left(2n + \frac{3}{2}\right) \hbar\omega_z, \quad (16)$$

where $n = 0, 1, \dots$. Inserting expansion (13) into Eq. (2), multiplying from the left with $\phi_{n'}^*(z)$, and integrating over z , results in

$$g_{1D}^- \hbar\omega_z \frac{d\phi_{n'}^*(0)}{dz} \left[\frac{d}{dz} \left(\sum_{n=0}^{\infty} c_n \phi_n(z) \right) \right]_{z \rightarrow 0^+} + c_{n'} (E_{n'}^{osc} - E_{1D}^-) = 0. \quad (17)$$

The coefficients $c_{n'}$ are hence of the form

$$c_{n'} = A \frac{\frac{d\phi_{n'}^*(0)}{dz}}{E_{n'}^{osc} - E_{1D}^-}, \quad (18)$$

where the constant A is independent of n' . Inserting this expression for the c_n into Eq. (17) leads to

$$\left[\frac{d}{dz} \left(\sum_{n=0}^{\infty} \frac{\frac{d\phi_n^*(0)}{dz} \phi_n(z)}{E_n^{osc} - E_{1D}^-} \right) \right]_{z \rightarrow 0^+} = -\frac{1}{g_{1D}^- \hbar\omega_z}. \quad (19)$$

If we define a non-integer quantum number ν through

$$E_{1D}^- = \left(2\nu + \frac{3}{2}\right) \hbar\omega_z, \quad (20)$$

and use expression (14) for the $\phi_n(z)$, Eq. (19) can be rewritten as

$$\frac{1}{\sqrt{\pi}} \left[\frac{d}{dz} \left\{ z \exp\left(-\frac{z^2}{2a_z^2}\right) \sum_{n=0}^{\infty} \frac{L_n^{(1/2)}(z^2/a_z^2)}{n - \nu} \right\} \right]_{z \rightarrow 0^+} = -\frac{a_z^3}{g_{1D}^-} \quad (21)$$

where the $z \rightarrow 0^+$ limit is well-behaved. Equation (21) can be evaluated using the identity

$$\sum_{n=0}^{\infty} \frac{L_n^{(1/2)}(z^2/a_z^2)}{n - \nu} = \Gamma(-\nu) U\left(-\nu, \frac{3}{2}, \frac{z^2}{a_z^2}\right), \quad (22)$$

and the known small z behavior of the hypergeometric function $U\left(-\nu, \frac{3}{2}, \frac{z^2}{a_z^2}\right)$ [31],

$$-\frac{1}{\pi} U\left(-\nu, \frac{3}{2}, \frac{z^2}{a_z^2}\right) \rightarrow -\frac{1}{\Gamma(-\nu)\Gamma(\frac{1}{2})} \left(\frac{z}{a_z}\right)^{-1} + \frac{1}{\Gamma(-\nu - \frac{1}{2})\Gamma(\frac{3}{2})} + O(z). \quad (23)$$

Using Eqs. (22) and (23) in Eq. (21), evaluating the derivative with respect to z , and then taking the $z \rightarrow 0^+$ limit, results in

$$-\frac{a_z^3}{g_{1D}^-} = -\frac{\sqrt{\pi}}{\Gamma(\frac{3}{2})} \frac{\Gamma(-\nu)}{\Gamma(-\nu - \frac{1}{2})}. \quad (24)$$

Replacing the non-integer quantum number ν [see Eq. (20)] by $E_{1D}^-/2\hbar\omega_z - 3/4$, we obtain the transcendental equation

$$\frac{g_{1D}^-}{a_z^3} = \frac{\Gamma(-\frac{E_{1D}^-}{2\hbar\omega_z} + \frac{1}{4})}{2\Gamma(-\frac{E_{1D}^-}{2\hbar\omega_z} + \frac{3}{4})}, \quad (25)$$

which allows the 1D odd-parity eigenenergies E_{1D}^- to be determined for a given interaction strength g_{1D}^- .

Solid lines in Fig. 1(b) show the 1D odd-parity eigenenergies E_{1D}^- , Eq. (25), as a function of g_{1D}^- . For $g_{1D}^- = 0$, the eigenenergies E_{1D}^- coincide with the odd-parity harmonic oscillator eigenenergies E_n^{osc} , Eq. (16); they increase for positive g_{1D}^- (“repulsive interactions”), and decrease for negative g_{1D}^- (“attractive interactions”).

Expansion of Eq. (25) to lowest order for large and negative eigenenergy (implying positive g_{1D}^-), $|E_{1D}^-| \rightarrow \infty$, results in

$$E_{1D}^- = -\frac{\hbar^2}{2\mu(a_{1D}^-)^2}, \quad (26)$$

where the 1D scattering length a_{1D}^- is defined analogously to a_{1D}^+ [with the superscript “+” in Eq. (7) replaced by the superscript “-”]. The 1D scattering length a_{1D}^- is related to the 1D coupling strength g_{1D}^- through

$$g_{1D}^- = a_{1D}^- a_z^2. \quad (27)$$

The energy given by Eq. (26) coincides with the binding energy of the 1D pseudo-potential $V_{pseudo}^-(z)$ without the confining potential. A dashed line in Fig. 1(b) shows E_{1D}^- , Eq. (26), while a dash-dotted line shows the expansion of Eq. (25) including the next order term.

In addition to the eigenenergies E_{1D}^- , we calculate the eigenfunctions Ψ_{1D}^- ,

$$\Psi_{1D}^-(z) \propto \frac{\Gamma(-\nu)}{\sqrt{a_z}} \frac{z}{a_z} \exp\left(-\frac{z^2}{2a_z^2}\right) U\left(-\nu, \frac{3}{2}, \frac{z^2}{a_z^2}\right). \quad (28)$$

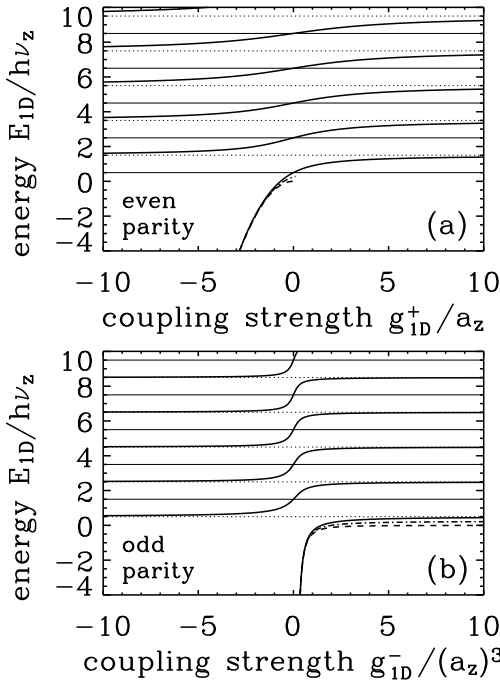


Figure 1: Solid lines in panel (a) show the relative even-parity energies E_{1D}^+ [Eq. (5)] calculated using the pseudo-potential $V_{pseudo}^+(z)$ as a function of g_{1D}^+ . Solid lines in panel (b) show the relative odd-parity energies E_{1D}^- [Eq. (25)] calculated using the pseudo-potential $V_{pseudo}^-(z)$ as a function of g_{1D}^- . Horizontal solid lines indicate the harmonic oscillator eigenenergies [with even parity in panel (a), and with odd parity in panel (b)]. Horizontal dotted lines indicate the asymptotic value of the eigenenergies E_{1D}^+ and E_{1D}^- for $g_{1D}^+ \rightarrow \pm\infty$ and $g_{1D}^- \rightarrow \pm\infty$, respectively. Dashed lines show the binding energies E_{1D}^+ , Eq. (6), in panel (a) and E_{1D}^- , Eq. (26), in panel (b) of the pseudo-potentials $V_{pseudo}^+(z)$ and $V_{pseudo}^-(z)$, respectively, without confinement. Dash-dotted lines show the expansion of Eq. (5) [panel (a)] and Eq. (25) [panel (b)] including the next order term.

Following steps similar to those outlined above, the logarithmic derivative at $z \rightarrow 0^+$ reduces to

$$\left[\frac{\frac{d\Psi_{1D}^-(z)}{dz}}{\Psi_{1D}^-(z)} \right]_{z \rightarrow 0^+} = -\frac{a_z^2}{g_{1D}^-}. \quad (29)$$

Equation (29) is an alternative representation of the 1D odd-parity pseudo-potential $V_{pseudo}^-(z)$ [28, 29, 30].

The even-parity eigenenergies E_{1D}^+ [Eq. (5)] and the odd-parity eigenenergies E_{1D}^- [Eq. (25)], as well as the logarithmic derivatives [Eqs. (9) and (29)] are identical if the coupling constants of $V_{pseudo}^+(z)$ and $V_{pseudo}^-(z)$ are chosen as follows,

$$g_{1D}^- = -\frac{a_z^4}{g_{1D}^+}. \quad (30)$$

This implies that even-parity energies E_{1D}^+ can be obtained by solving the 1D Schrödinger equation, Eq. (2), for H_{1D} given

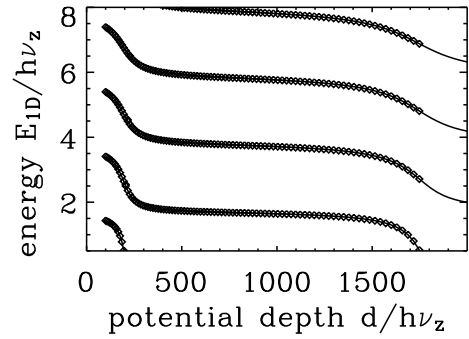


Figure 2: Relative odd-parity eigenenergies E_{1D}^- for two particles under 1D harmonic confinement as a function of the well depth d . Solid lines show the eigenenergies obtained by solving the 1D Schrödinger equation, Eq. (2), for the Hamiltonian given in Eq. (3) numerically using a short-range model potential, Eq. (31), for a series of well depths d . Symbols show the eigenenergies obtained for the pseudo-potential $V_{pseudo}^-(z)$, taking the energy-dependence of the 1D coupling constant g_{1D}^- into account, $g_{1D}^- = g_{1D}^-(E_{sc})$ (see text).

by Eq. (3) with $V(z) = V_{pseudo}^-(z)$ [and vice versa, odd-parity energies E_{1D}^- can be obtained by solving the 1D Schrödinger equation with $V(z) = V_{pseudo}^+(z)$]. Our analytical treatment of two 1D particles under external confinement thus confirms the Fermi-Bose duality for two 1D particles under harmonic confinement [25, 26, 27, 28, 29].

C. Comparison with shape-dependent 1D atom-atom potential

To benchmark the applicability of the odd-parity pseudo-potential $V_{pseudo}^-(z)$ to two 1D atoms under harmonic confinement, we solve the 1D Schrödinger equation, Eq. (2), for the Hamiltonian given by Eq. (3) numerically for the shape-dependent Morse potential $V_{morse}(z)$,

$$V_{morse}(z) = de^{-\alpha(z-z_0)} \left[e^{-\alpha(z-z_0)} - 2 \right]. \quad (31)$$

Our numerical calculations are performed for a fixed range parameter z_0 , $z_0 = 11.65$ a.u., and for $\alpha = 0.35$ a.u.; these parameters roughly approximate the 3D Rb₂ triplet potential [32]. The angular trapping frequency ω_z is fixed at 10^{-9} a.u. ($2\pi\nu_z = \omega_z$), and the atom mass m at that of the ⁸⁷Rb atom, implying an oscillator length a_z of 112.5 a.u., and hence a fairly tightly trapped atom pair. To investigate potentials with different 1D scattering properties, we choose depth parameters d for which the 1D Morse potential supports between zero and two 1D odd-parity bound states. Solid lines in Fig. 2 show the resulting 1D odd-parity eigenenergies E_{1D}^- obtained numerically as a function of d . The corresponding eigenstates have “gas-like character”, that is, these states would correspond to continuum states if the confining potential was absent.

To compare the odd-parity eigenenergies obtained numerically for the Morse potential $V_{\text{morse}}(z)$ with those obtained for the odd-parity pseudo-potential $V_{\text{pseudo}}^-(z)$, we follow Refs. [14, 15]. We first perform scattering calculations for the 1D Morse potential (no confinement) as a function of the relative scattering energy E_{sc} for various depths d , which provide, for a given d , the energy-dependent 1D scattering length $a_{1D}^-(E_{sc})$, where $a_{1D}^-(E_{sc}) = -\tan(\delta_{1D}^-(k))/k$. Using the relation between the 1D scattering length a_{1D}^- and the 1D coupling strength g_{1D}^- , Eq. (27), we then solve the transcendental equation (25) self-consistently for E_{1D}^- .

Diamonds in Fig. 2 show the resulting odd-parity eigenenergies E_{1D}^- for two 1D particles under harmonic confinement interacting through the odd-parity energy-dependent pseudo-potential $V_{\text{pseudo}}^-(z)$ with $g_{1D}^- = g_{1D}^-(E_{sc})$. Excellent agreement between these eigenenergies and those obtained for the Morse potential (solid lines) is visible for all well depths d . We emphasize that this agreement depends crucially on the usage of *energy-dependent* 1D coupling constants. In summary, Fig. 2 illustrates that the odd-parity pseudo-potential $V_{\text{pseudo}}^-(z)$ provides a good description of the eigenstates of two spin-polarized 1D fermions under harmonic confinement for all interaction strengths, including $g_{1D}^- \rightarrow \pm\infty$.

III. TWO INTERACTING 3D PARTICLES UNDER HARMONIC CONFINEMENT

Consider two 3D particles with mass m and coordinates \vec{r}_1 and \vec{r}_2 , respectively, confined by the potential $V_{\text{trap}}(\vec{r}_1, \vec{r}_2)$,

$$V_{\text{trap}}(\vec{r}_1, \vec{r}_2) = \frac{1}{2}\mu\omega_{ho}^2(\vec{r}_1^2 + \vec{r}_2^2), \quad (32)$$

where ω_{ho} denotes the angular trapping frequency of the harmonic 3D confinement. The corresponding Schrödinger equation decouples into a center of mass part, whose solution can be readily written down, and into a relative part,

$$H_{3D} = H_{3D}^{osc} + V(\vec{r}). \quad (33)$$

Here, \vec{r} denotes the relative coordinate vector ($\vec{r} = \vec{r}_2 - \vec{r}_1$), $V(\vec{r})$ the atom-atom interaction potential, and H_{3D}^{osc} the 3D harmonic oscillator Hamiltonian,

$$H_{3D}^{osc} = -\frac{\hbar^2}{2\mu}\nabla_{\vec{r}}^2 + \frac{1}{2}\mu\omega_{ho}^2\vec{r}^2. \quad (34)$$

The corresponding Schrödinger equation for the relative coordinate reads

$$H_{3D}\Psi_{3D}(\vec{r}) = E_{3D}\Psi_{3D}(\vec{r}). \quad (35)$$

Section III A briefly reviews Fermi Huang's regularized s -wave pseudo-potential, while Section III B solves Eq. (35) for a regularized p -wave zero-range potential analytically. To illustrate the applicability of this p -wave pseudo-potential, Section III C compares the resulting relative eigenenergies E_{3D} for two particles under harmonic confinement with those obtained numerically for a shape-dependent short-range model potential.

A. Review of 3D pseudo-potential treatment: s -wave

Using Fermi-Huang's regularized s -wave ($l = 0$) pseudo-potential $V_{\text{pseudo}}^{l=0}(\vec{r})$ [9, 11],

$$V_{\text{pseudo}}^{l=0}(\vec{r}) = \frac{2\pi\hbar^2}{\mu}a_s\delta^{(3)}(\vec{r})\frac{\partial}{\partial r}r, \quad (36)$$

where $\delta^{(3)}(\vec{r})$ denotes the radial component of the 3D δ -function,

$$\delta^{(3)}(\vec{r}) = \frac{1}{4\pi r^2}\delta^{(1)}(r), \quad (37)$$

and a_s the 3D s -wave scattering length, Busch *et al.* [12] derive a transcendental equation for the relative 3D eigenenergies E_{3D} ,

$$\frac{a_s}{a_{ho}} = \frac{\Gamma(-\frac{E_{3D}}{2\hbar\omega_{ho}} + \frac{1}{4})}{2\Gamma(-\frac{E_{3D}}{2\hbar\omega_{ho}} + \frac{3}{4})}. \quad (38)$$

Here, a_{ho} denotes the oscillator length, $a_{ho} = \sqrt{\hbar/(\mu\omega_{ho})}$. Solid lines in Fig. 3(a) show the s -wave energies E_{3D} as a function of a_s . For large and negative E_{3D} (and hence positive a_s), an expansion of Eq. (38) to lowest order results in

$$E_{3D} = -\frac{\hbar^2}{2\mu(a_s)^2}, \quad (39)$$

which corresponds to the binding energy of $V_{\text{pseudo}}^{l=0}(\vec{r})$ without the confining potential. A dashed line in Fig. 1 shows the energy given by Eq. (39), while a dash-dotted line shows the expansion of Eq. (38) including the next higher order term.

Since only s -wave wave functions have a non-vanishing amplitude at $r = 0$, Fermi-Huang's regularized pseudo-potential leads exclusively to s -wave scattering (no other partial waves are scattered). Equation (38) hence applies to two ultracold bosons under external confinement, for which higher even partial waves, such as d - or g -waves, are negligible.

Recall that the irregular solution with $l = 0$ diverges as r^{-1} . The so-called regularization operator $\frac{\partial}{\partial r}r$ of the pseudo-potential $V_{\text{pseudo}}^s(\vec{r})$, Eq. (36), cures this divergence. The solutions $\Psi_{3D}(\vec{r})$ of two particles under external confinement obey the boundary condition

$$\left[\frac{\frac{\partial}{\partial r}(r\Psi_{3D}(\vec{r}))}{r\Psi_{3D}(\vec{r})} \right]_{r \rightarrow 0} = -\frac{1}{a_s}; \quad (40)$$

this boundary condition is an alternative representation of $V_{\text{pseudo}}^{l=0}(\vec{r})$.

B. Analytical 3D pseudo-potential treatment: p -wave

The importance of angle-dependent p -wave interactions has recently been demonstrated experimentally for two potassium atoms in the vicinity of a magnetic field-dependent

p -wave Feshbach resonance [33]. Here, we use a p -wave pseudo-potential to model *isotropic* atom-atom interactions; treatment of anisotropic interactions is beyond the scope of this paper.

We use the following p -wave pseudo-potential $V_{pseudo}^{l=1}(\vec{r})$,

$$V_{pseudo}^{l=1}(\vec{r}) = g_1 \overleftarrow{\nabla_{\vec{r}}} \delta^{(3)}(\vec{r}) \nabla_{\vec{r}} \rightarrow \frac{1}{2} \frac{\partial^2}{\partial r^2} r^2, \quad (41)$$

where the coupling strength g_1 ‘‘summarizes’’ the scattering properties of the original shape-dependent atom-atom interaction potential [34, 35],

$$g_1 = \frac{6\pi\hbar^2}{\mu} V_p. \quad (42)$$

Here, V_p denotes the p -wave scattering volume [4],

$$V_p = \lim_{k \rightarrow 0} -\frac{\tan(\delta_p(k))}{k^3}, \quad (43)$$

δ_p the p -wave phase shift, and k the relative 3D collision wave vector. Similarly to the 1D odd-parity pseudo-potential $V_{pseudo}^-(z)$, the first gradient $\nabla_{\vec{r}}$ with respect to the relative vector \vec{r} acts to the left, while the second one acts to the right,

$$g_1 \int [\nabla_{\vec{r}} \phi^*(\vec{r})] \delta^{(3)}(\vec{r}) \left[\nabla_{\vec{r}} \left\{ \frac{1}{2} \frac{\partial^2}{\partial r^2} (r^2 \chi(\vec{r})) \right\} \right] d^3\vec{r} = \int \phi^*(\vec{r}) V_{pseudo}^{l=1}(\vec{r}) \chi(\vec{r}) d^3\vec{r} \quad (44)$$

Just as the s -wave pseudo-potential $V_{pseudo}^{l=0}(\vec{r})$ does not couple to partial waves with $l \neq 0$, the p -wave pseudo-potential $V_{pseudo}^{l=1}(\vec{r})$ does not couple to partial waves with $l \neq 1$ [36]. Pseudo-potentials of the form $g_1 \overleftarrow{\nabla_{\vec{r}}} \delta^{(3)}(\vec{r}) \nabla_{\vec{r}} \rightarrow$ have been used by a number of researchers before [34, 35, 36, 37]; discrepancies regarding the proper value of the coefficient g_1 , however, exist (see, e.g., Ref. [36]). Here, we introduce the regularization operator $\frac{1}{2} \frac{\partial^2}{\partial r^2} r^2$ [Eq. (41)], which eliminates divergencies that would arise otherwise from the irregular p -wave solution (which diverges as r^{-2}). A similar regularization operator has been proposed by Huang and Yang in 1957 [11]; they, however, use it in conjunction with a coupling parameter g_1 different from that given by Eq. (42). By comparing with numerical results for a shape-dependent model potential, we show that the pseudo-potential $V_{pseudo}^{l=1}(\vec{r})$ describes the scattering behaviors of two spin-aligned 3D fermions properly (see Sec. III C).

To determine the relative eigenenergies E_{3D} of two spin-polarized 3D fermions under harmonic confinement analytically, we expand the 3D wave function $\psi_{3D}(\vec{r})$ for fixed angular momentum, $l = 1$, in *continuous* harmonic oscillator eigen functions $\phi_{nlm_l}(\vec{r})$,

$$\psi_{3D}(\vec{r}) = \sum_{nm_l} c_{nm_l} \phi_{nlm_l}(\vec{r}), \quad (45)$$

where the c_{nm_l} denote expansion coefficients. The $\phi_{nlm_l}(\vec{r})$ depend on the principal quantum number n , the angular momentum quantum number l , and the projection quantum number

m_l ,

$$H_{3D}^{osc} \phi_{nlm_l}(\vec{r}) = E_{nl}^{osc} \phi_{nlm_l}(\vec{r}) \quad (46)$$

and

$$E_{nl}^{osc} = \left(2n + l + \frac{3}{2} \right) \hbar \omega_{ho}, \quad (47)$$

where $n = 0, 1, \dots$; $l = 0, 1, \dots, n-1$; and $m_l = 0, \pm 1, \dots, \pm l$. The $\phi_{nlm_l}(\vec{r})$ can be written in spherical coordinates $[\vec{r} = (r, \vartheta, \varphi)]$,

$$\phi_{nlm_l}(\vec{r}) = \sqrt{4\pi} R_{nl}(r) Y_{lm_l}(\vartheta, \varphi), \quad (48)$$

where the $Y_{lm_l}(\vartheta, \varphi)$ denote spherical harmonics and the $R_{nl}(r)$ are given by

$$R_{nl}(r) = \sqrt{\frac{2^l}{(2l+1)!! \sqrt{\pi^3} L_n^{(l+1/2)}(0) a_{ho}^3}} \times \left(\frac{r}{a_{ho}} \right)^l \exp\left(-\frac{r^2}{2a_{ho}^2}\right) L_n^{(l+1/2)}\left(\frac{r^2}{a_{ho}^2}\right), \quad (49)$$

with

$$(2l+1)!! = 1 \cdot 3 \cdot \dots \cdot (2l+1). \quad (50)$$

The normalizations of $R_{nl}(r)$ and $Y_{lm_l}(\vartheta, \varphi)$ are chosen as

$$\int_0^{2\pi} \int_0^\pi |Y_{lm_l}(\vartheta, \varphi)|^2 \sin \vartheta d\vartheta d\varphi = 1 \quad (51)$$

and

$$\int_0^\infty |R_{nl}(r)|^2 r^2 dr = \frac{1}{4\pi}. \quad (52)$$

If we plug expansion (45) into the 3D Schrödinger equation, Eq. (35), for the Hamiltonian given by Eq. (33) with $V(\vec{r}) = V_{pseudo}^{l=1}(\vec{r})$, multiply from the left with $\phi_{n'l'm'_l}^*(\vec{r})$ [with $l = 1$], and integrate over \vec{r} , we obtain an expression for the coefficients $c_{n'l'm'_l}$,

$$c_{n'l'm'_l} (E_{n'l}^{osc} - E_{3D}) = -g_1 [\nabla_{\vec{r}} R_{n'l}^*(0)] \cdot \left[\nabla_{\vec{r}} \left\{ \frac{1}{2} \frac{\partial^2}{\partial r^2} \left(r^2 \sum_{nm_l} c_{nm_l} R_{nl}(r) \right) \right\} \right]_{r \rightarrow 0} \quad (53)$$

where

$$\nabla_{\vec{r}} R_{n'l}^*(0) = [\nabla_{\vec{r}} R_{n'l}^*(r)]_{r=0}. \quad (54)$$

In deriving Eq. (53), we use that

$$\nabla_{\vec{r}} [R_{nl}(r) Y_{lm_l}(\vartheta, \varphi)] = [\nabla_{\vec{r}} R_{nl}(r)] Y_{lm_l}(\vartheta, \varphi) + R_{nl}(r) [\nabla_{\vec{r}} Y_{lm_l}(\vartheta, \varphi)], \quad (55)$$

where the second term on the right-hand side goes to zero in the $r \rightarrow 0$ limit. Since the gradients $\nabla_{\vec{r}}$ in Eq. (53) act on

arguments that depend solely on r , we can replace them by $\hat{e}_r \frac{\partial}{\partial r}$ (where \hat{e}_r denotes the unit vector in the r -direction),

$$c_{n'l} (E_{n'l}^{osc} - E_{3D}) = -g_1 \frac{\partial R_{n'l}^*(0)}{\partial r} \left[\frac{1}{2} \frac{\partial^3}{\partial r^3} \left(r^2 \sum_{n=0}^{\infty} c_{nm'l} R_{nl}(r) \right) \right]_{r \rightarrow 0}. \quad (56)$$

Equation (56) implies that the coefficients $c_{n'l}$ are of the form

$$c_{n'l} = A \frac{\frac{\partial R_{n'l}^*(0)}{\partial r}}{E_{n'l}^{osc} - E_{3D}}, \quad (57)$$

where A is a constant independent of n' . Plugging Eq. (57) into Eq. (56) results in an implicit expression for the 3D energies E_{3D} ,

$$\left[\frac{1}{2} \frac{\partial^3}{\partial r^3} \left(r^2 \sum_{n=0}^{\infty} \frac{\frac{\partial R_{nl}^*(0)}{\partial r} R_{nl}(r)}{E_{nl}^{osc} - E_{3D}} \right) \right]_{r \rightarrow 0} = -\frac{1}{g_1}. \quad (58)$$

To simplify the infinite sum over n , we use expression (49) for the $R_{nl}(r)$, and introduce a non-integer quantum number ν ,

$$E_{3D} = \left(2\nu + l + \frac{3}{2} \right) \hbar\omega_{ho}. \quad (59)$$

For $l = 1$, we obtain

$$\frac{1}{3\sqrt{\pi^3}} \left[\frac{1}{2} \frac{\partial^3}{\partial r^3} \left(\exp\left(-\frac{r^2}{2a_{ho}^2}\right) r^3 \sum_{n=0}^{\infty} \frac{L_n^{(3/2)}(r^2/a_{ho}^2)}{n-\nu} \right) \right]_{r \rightarrow 0} = -\frac{\hbar\omega_{ho} a_{ho}^5}{g_1} \quad (60)$$

Using the identity

$$\sum_{n=0}^{\infty} \frac{L_n^{(3/2)}(r^2/a_{ho}^2)}{n-\nu} = \Gamma(-\nu) U\left(-\nu, \frac{5}{2}, \frac{r^2}{a_{ho}^2}\right), \quad (61)$$

the infinite sum in Eq. (60) can be rewritten,

$$\frac{\Gamma(-\nu)}{3\sqrt{\pi^3}} \left[\frac{1}{2} \frac{\partial^3}{\partial r^3} \left(\exp\left(-\frac{r^2}{2a_{ho}^2}\right) r^3 U\left(-\nu, \frac{5}{2}, \frac{r^2}{a_{ho}^2}\right) \right) \right]_{r \rightarrow 0} = -\frac{\hbar\omega_{ho} a_{ho}^5}{g_1} \quad (62)$$

where the $r \rightarrow 0$ limit is, as discussed above, due to the regularization operator of $V_{pseudo}^{l=1}(\vec{r})$ well behaved. Expression (62) can be evaluated using the known small r behavior of the hypergeometric function $U(-\nu, \frac{5}{2}, \frac{r^2}{a_{ho}^2})$ [31],

$$\frac{1}{\pi} \Gamma(-\nu) U\left(-\nu, \frac{5}{2}, \frac{r^2}{a_{ho}^2}\right) \rightarrow -\left(\frac{r}{a_{ho}}\right)^{-3} \frac{1}{\Gamma(-\frac{1}{2})} - \left(\frac{r}{a_{ho}}\right)^{-1} \frac{(2\nu+3)}{\Gamma(-\frac{1}{2})} + \frac{\Gamma(-\nu)}{\Gamma(-\nu-\frac{3}{2})\Gamma(\frac{5}{2})} + \mathcal{O}(r). \quad (63)$$

If we insert expansion (63) into Eq. (62), evaluate the derivatives, and take the $r \rightarrow 0$ limit, we find

$$-\frac{\hbar\omega_{ho} a_{ho}^5}{g_1} = \frac{1}{\sqrt{\pi}} \frac{\Gamma(-\nu)}{\Gamma(-\nu-\frac{3}{2})\Gamma(\frac{5}{2})}. \quad (64)$$

Using Eqs. (42) and (59), we obtain our final expression for the relative eigenenergies E_{3D} for $l = 1$,

$$\frac{V_p}{a_{ho}^3} = -\frac{\Gamma(-\frac{E_{3D}}{2\hbar\omega_{ho}} - \frac{1}{4})}{8\Gamma(-\frac{E_{3D}}{2\hbar\omega_{ho}} + \frac{5}{4})}. \quad (65)$$

Solid lines in Fig. 3(b) show the relative 3D eigenenergies E_{3D} , Eq. (65), for two spin-polarized fermions under external harmonic confinement interacting through the zero-range pseudo-potential $V_{pseudo}^{l=1}(\vec{r})$ as a function of the 3D scattering volume V_p . For vanishing coupling strength g_1 (or equivalently, for $V_p = 0$), E_{3D} coincides with the $l = 1$ harmonic oscillator eigenenergy. As V_p increases [decreases], E_{3D} increases [decreases].

Expansion of Eq. (65) for a large and negative eigenenergy (and hence negative V_p), $|E_{3D}| \rightarrow \infty$, results in

$$E_{3D} = -\frac{\hbar^2}{2\mu(V_p)^{2/3}}, \quad (66)$$

which agrees with the binding energy of $V_{pseudo}^{l=1}(\vec{r})$ without the confinement potential. A dashed line in Fig. 3(b) shows this binding energy, while a dash-dotted line shows the expansion of Eq. (65) including the next higher order. Compared to the eigenenergy of the system without confinement, Eq. (66), the lowest eigenenergy given by Eq. (65) is downshifted. This downshift is somewhat counterintuitive, and contrary to the s -wave case.

In addition to the eigenenergies E_{3D} of two atoms with $l = 1$ under harmonic confinement, we determine the corresponding eigenfunctions $\Psi_{3D}(\vec{r})$,

$$\Psi_{3D}(\vec{r}) \propto \frac{\Gamma(-\nu)}{(a_{ho})^{3/2}} \frac{r}{a_{ho}} \exp\left(-\frac{r^2}{2a_{ho}^2}\right) U\left(-\nu, \frac{5}{2}, \frac{r^2}{a_{ho}^2}\right), \quad (67)$$

which lead to the well-behaved boundary condition

$$\left[\frac{\frac{\partial^3}{\partial r^3} \left(\frac{1}{2} r^2 \Psi_{3D}(\vec{r}) \right)}{r^2 \Psi_{3D}(\vec{r})} \right]_{r \rightarrow 0} = -\frac{1}{V_p}. \quad (68)$$

This boundary condition is an alternative representation of the pseudo-potential $V_{pseudo}^{l=1}(\vec{r})$, and depends on only one parameter, that is, the scattering volume V_p . This is in contrast to earlier work [19, 20], which treated a boundary condition similar to Eq. (68) but evaluated the left hand side at a finite value of r , i.e., at $r = r_e$. The boundary condition containing the finite parameter r_e cannot be mapped to a zero-range pseudo-potential. References [38, 39, 40] discuss alternative derivations and representations of boundary condition (68).

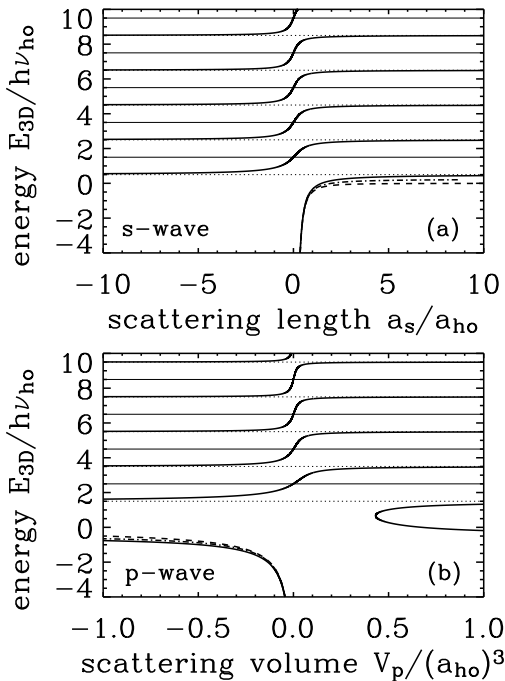


Figure 3: Solid lines in panel (a) show the relative s -wave energies E_{3D} [Eq. (38)] calculated using the pseudo-potential $V_{pseudo}^{l=0}(\vec{r})$ as a function of the scattering length a_s . Solid lines in panel (b) show the relative p -wave energies E_{3D} [Eq. (65)] calculated using the pseudo-potential $V_{pseudo}^{l=1}(\vec{r})$ as a function of the scattering volume V_p . Horizontal solid lines indicate the harmonic oscillator eigenenergies [for $l=0$ in panel (a), and for $l=1$ in panel (b)]. Horizontal dotted lines indicate the asymptotic eigenenergies E_{3D} [for $a_s \rightarrow \pm\infty$ in panel (a), and for $V_p \rightarrow \pm\infty$ in panel (b)]. Dashed lines show the binding energies, Eq. (39) in panel (a) and Eq. (66) in panel (b), of the pseudo-potentials $V_{pseudo}^{l=0}(\vec{r})$ and $V_{pseudo}^{l=1}(\vec{r})$, respectively, without confinement. Dash-dotted lines show the expansion of Eq. (38) [panel (a)] and Eq. (65) [panel (b)] including the next order term.

C. Comparison with shape-dependent 3D atom-atom potential

To benchmark our p -wave pseudo-potential treatment of two spin-polarized 3D fermions under harmonic confinement, we solve the 3D Schrödinger equation, Eq. (35), for the Hamiltonian given by Eq. (33) numerically for the shape-dependent Morse potential $V_{morse}(r)$, Eq. (31) with z replaced by r and z_0 replaced by r_0 . As in Sec. II C, our numerical calculations are performed for $r_0 = 11.65$ a.u., $\alpha = 0.35$ a.u., $\omega_{ho} = 10^{-9}$ a.u. ($2\pi\nu_{ho} = \omega_{ho}$), and $m = m(^{87}\text{Rb})$. The well depth d is chosen such that the 3D Morse potential supports between zero and two $l=1$ bound states. Solid lines in Fig. 4 show the resulting 3D eigenenergies E_{3D} with $l=1$ obtained numerically as a function of the depth d .

To compare the $l=1$ eigenenergies obtained numerically for the Morse potential $V_{morse}(r)$ with those obtained for the p -wave pseudo-potential $V_{pseudo}^{l=1}(\vec{r})$, we follow the procedure outlined in Sec. II C, that is, we first determine the energy-

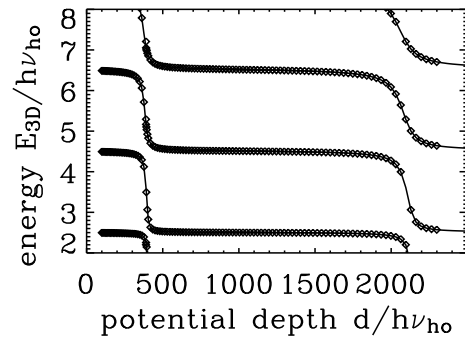


Figure 4: Relative 3D eigenenergies E_{3D} with $l=1$ for two spin-polarized fermions under 3D harmonic confinement as a function of the well depth d . Solid lines show the eigenenergies obtained by solving the 3D Schrödinger equation, Eq. (35), for the Hamiltonian given in Eq. (33) numerically for a short-range model potential, Eq. (31) with z replaced by r and z_0 replaced by r_0 , for a series of well depths d . Symbols show the eigenenergies obtained for the pseudo-potential $V_{pseudo}^{l=1}(\vec{r})$, taking the energy-dependence of the 3D scattering volume V_p into account, $V_p = V_p(E_{sc})$ (see text).

dependent free-space scattering volume $V_p(E_{sc})$, $V_p(E_{sc}) = -\tan(\delta_p(k))/k^3$, for the 3D Morse potential (no confinement) as a function of the relative scattering energy E_{sc} for various well depths d . We then solve the transcendental equation (65) self-consistently for E_{3D} . Diamonds in Fig. 4 show the resulting $l=1$ eigenenergies E_{3D} for two 3D particles under harmonic confinement interacting through the $l=1$ energy-dependent pseudo-potential $V_{pseudo}^{l=1}(\vec{r})$ with $V_p = V_p(E_{sc})$. Excellent agreement between these eigenenergies and those obtained for the Morse potential (solid lines) is visible for all well depths d . We emphasize that this agreement depends crucially on the usage of *energy-dependent* 3D scattering volumes. Figure 4 illustrates that the p -wave pseudo-potential $V_{pseudo}^{l=1}(\vec{r})$ describes p -wave scattering processes properly.

IV. SUMMARY

We determined the eigenspectrum for two 1D particles under harmonic confinement interacting through a momentum-dependent zero-range potential. This pseudo-potential acts only on states with odd-parity, and is hence applicable to the scattering between two spin-polarized 1D fermions. We showed that a basis set expansion in continuous functions can be used to determine the eigenenergies and discontinuous eigenfunctions of two 1D particles under harmonic confinement interacting through the odd-parity pseudo-potential $V_{pseudo}^-(z)$. Our divergence-free treatment confirms the Fermi-Bose duality in 1D for two particles.

We also determined an implicit expression for the eigenenergies E_{3D} , Eq. (65), and eigenfunctions $\psi_{3D}(\vec{r})$, Eq. (67), of two spin-polarized 3D fermions under harmonic confinement interacting through a momentum-dependent zero-range

potential. Similar to studies of two atoms with $l = 0$ [13, 14, 15, 16], our analytical expressions might be useful in understanding the behavior of two confined spin-aligned fermions, including physics near Feshbach resonances. The p -wave pseudo-potential used in our study contains derivative operators as well as a regularization operator; the former is needed to construct a true zero-range potential (since $l = 1$ solutions go to zero as r approaches zero, see above) while the latter is needed to eliminate divergencies of the irregular p -wave solution (which diverges as r^{-2}). We showed that our zero-range potential $V_{pseudo}^{l=1}(\vec{r})$ imposes a boundary condition at $r = 0$, Eq. (68), which depends on a single atomic physics parameter, that is, the scattering volume V_p . This boundary condition is an alternative representation of $V_{pseudo}^{l=1}(\vec{r})$.

Similarly to Fermi-Huang's regularized s -wave pseudo-potential, the p -wave pseudo-potential used here might find

applications in developing effective many-body theories for ultracold spin-polarized Fermi gases. Such theories will have to carefully investigate how to implement renormalization procedures needed in numerical calculations.

Note added: After submission of this paper we became aware of a related study by Stock *et al.*, see quant-ph/0405153, which derives Eq. (65) starting with a pseudo-potential expressed as the limit of a δ -shell.

Acknowledgments

This work was supported by the NSF under grant PHY-0331529. Discussions with Dimitri Fedorov, Marvin Girardeau and Brian Granger are gratefully acknowledged.

-
- [1] F. Dalfovo, S. Giorgini, L. P. Pitaevskii, and S. Stringari, Rev. Mod. Phys. **71**, 463 (1999).
 - [2] M. H. Anderson *et al.*, Science **269**, 198 (1995).
 - [3] C. A. Regal, C. Ticknor, J. L. Bohn, and D. S. Jin, Phys. Rev. Lett. **90**, 053201 (2003).
 - [4] H. Suno, B. D. Esry, and C. H. Greene, Phys. Rev. Lett. **90**, 053202 (2003).
 - [5] E. D. C. Mattis, *The many-body problem: An encyclopedia of exactly solved models in one dimension* (World Scientific, Singapore, 1993).
 - [6] M. Olshanii, Phys. Rev. Lett. **81**, 938 (1998).
 - [7] Y. N. Demkov and V. N. Ostrovskii, *Zero-range potentials and their applications in atomic physics* (New York, Plenum, New York and London, 1988).
 - [8] S. Albeverio, F. Gesztesy, R. Høegh-Krohn, and H. Holden, *Solvable models in quantum mechanics* (Springer, New York, 1988).
 - [9] E. Fermi, Nuovo Cimento **11**, 157 (1934).
 - [10] G. Breit and P. R. Zilsel, Phys. Rev. **71**, 232 (1947).
 - [11] K. Huang and C. N. Yang, Phys. Rev. **105**, 767 (1957).
 - [12] T. Busch, B.-G. Englert, K. Rzȃzewski, and M. Wilkens, Foundations of Phys. **28**, 549 (1998).
 - [13] E. Tiesinga, C. J. Williams, and P. S. Julienne, Phys. Rev. A **61**, 063416 (2000).
 - [14] D. Blume and C. H. Greene, Phys. Rev. A **65**, 043613 (2002).
 - [15] E. L. Bolda, E. Tiesinga, and P. S. Julienne, Phys. Rev. A **66**, 013403 (2002).
 - [16] B. Borca, D. Blume, and C. H. Greene, New J. Phys. **5**, 111 (2003).
 - [17] E. A. Donley, N. R. Claussen, S. T. Thompson, and C. E. Wieman, Nature **417**, 529 (2002).
 - [18] K. Huang, Int. J. Mod. Phys. A **4**, 1037 (1989).
 - [19] Y. N. Demkov and G. F. Drukarev, Sov. Phys. JETP **54**, 650 (1981).
 - [20] M. V. Frolov, N. L. Manakov, E. A. Pronin, and A. F. Starace, Phys. Rev. Lett. **91**, 053003 (2003).
 - [21] J. Reichel, W. Hansell, and T. W. Hansch, Phys. Rev. Lett. **83**, 3398 (1999).
 - [22] D. Muller *et al.*, Phys. Rev. Lett. **83**, 5194 (1999).
 - [23] A. Gorlitz *et al.*, Phys. Rev. Lett. **87**, 130402 (2001).
 - [24] K. Wodkiewicz, Phys. Rev. A **43**, 68 (1991).
 - [25] T. Cheon and T. Shigehara, Phys. Lett. A **243**, 111 (1998).
 - [26] T. Cheon and T. Shigehara, Phys. Lett. Rev. **82**, 2536 (1999).
 - [27] B. E. Granger and D. Blume, Phys. Rev. Lett. **92**, 133202 (2004).
 - [28] M. D. Girardeau and M. Olshanii, cond-mat/0309396.
 - [29] H. Grosse, E. Langmann, and C. Paupfler, math-ph/0401003.
 - [30] M. D. Girardeau and M. Olshanii, cond-mat/0401402.
 - [31] M. Abramowitz and I. E. Stegun, *Eds.*, *Handbook of mathematical functions, 10th edition; entry 13.1.3* (Department of Commerce, 1972).
 - [32] B. D. Esry and C. H. Greene, Phys. Rev. A **60**, 1451 (1999).
 - [33] C. Ticknor, C. A. Regal, D. S. Jin, and J. L. Bohn, Phys. Rev. A **69**, 042712 (2004).
 - [34] A. Omont, Journal de Physique **38**, 1343 (1977).
 - [35] E. L. Hamilton, C. H. Greene, and H. R. Sadeghpour, J. Phys. B **35**, L119 (2002).
 - [36] R. Roth and H. Feldmeier, Phys. Rev. A **64**, 043603 (2001).
 - [37] E. L. Hamilton, Ph.D. thesis, University of Colorado (2003).
 - [38] S. P. Andreev, B. M. Karnakov, V. D. Mur, and V. A. Polunin, Sov. Phys. JETP **59**, 506 (1984).
 - [39] S. P. Andreev, B. M. Karnakov, and V. D. Mur, Theor. Math. Phys. **64**, 838 (1986).
 - [40] A. S. Baltenkov, Phys. Lett. A **268**, 92 (2000).